Feedback Linearization with Intelligent Disturbance Observer for Autonomous Quadrotor with Time-varying Disturbance

Izzuddin M. Lazim, Abdul Rashid Husain, Mohd Ariffanan Mohd Basri and Nurul Adilla Mohd Subha

***Abstract*—The presence of disturbances during flight may destabilize the quadrotor control and could compromise the designated mission. This paper proposes an improved quadrotor flight control in the presence of wind disturbances where the performance will be more robust in many flight conditions. This is achieved by integrating artificial intelligence (AI) technique with disturbance observer-based feedback linearization to improve the disturbance approximation and compensation. The AI technique via radial basis function neural network (RBFNN) is implemented to compensate the bounded estimation error produced by the disturbance observer. The weights of the neural network are tuned online with no prior training required. Simulation results demonstrate the effectiveness and feasibility of the proposed technique.**

***Index Terms*—Disturbance observer, feedback linearization, neural network, quadcopter**

I. Introduction

Unmanned aerial vehicle (UAV) has received much attention in recent decades due to the versatility and usefulness of the aircraft in various sectors including e-commerce, energy, transportation, and civil for applications such as delivery, inspection, and surveillance. One of the popular types of UAV is quadrotor that has a simple structure, and the ability to take off and land vertically [1]. However, quadrotor is inherently unstable and has a complex dynamic model. In addition, it is also very susceptible to external disturbances such as wind gust [2]. Therefore, a good control approach is needed for the quadrotor to fly autonomously, and to accomplish the designated tasks effectively.

In the literature, a considerable large number of works have proposed quadrotor control algorithms based on linear control designs such as Proportional-Integral-Derivative (PID) [3], [4] and Linear Quadratic Regulator (LQR) [5], [6]. The linear controllers are derived based on the linearized quadrotor model around some nominal operating condition point, e.g. hovering condition [7]. Even though the linear control schemes have proven the capability in this application, the performance is only valid around the nominal operating point.

In contrast to the linearization approach at the operating conditions, nonlinear control based on feedback linearization technique produces a linear model representation of the nonlinear quadrotor model over a large set of operating conditions [8]. Then, various linear control algorithms can be used in the outer-loop to stabilize the transformed linear system. In [9], static feedback linearization is implemented to obtain a linear quadrotor model for formation control problem. In [10]–[12], dynamic feedback linearization is employed to obtain an integrator model of the quadrotor. These works have widened the potential applications of various linear controllers that can benefit from the resultant linearized quadrotor model. However, feedback linearization approach is sensitive to disturbances (e.g. wind) which may render instability to the system.

Adaptive or robust techniques are the common control methods used to improve the robustness of feedback linearization, e.g. [13], [14]. Nevertheless, these methods cause the closed-loop transient response to be shaped by the adaptive or robust control component instead of the nominal linear model. In addition, adaptive or robust control techniques are based on feedback control which may not react directly and fast enough in the presence of strong disturbances [15]. To overcome these limitations, researchers have proposed a method of so-called active anti-disturbance control (AADC) technique.

In contrast to the adaptive or robust methods, AADC technique reacts directly to the disturbances by feedforward compensation control design using measurements or disturbance estimations via disturbance observer. In [16], a feedback linearization-based controller with a high order sliding mode observer is proposed for trajectory tracking of a quadrotor in the presence of sinusoidal disturbances. In [17], feedback linearization with an observer is implemented to estimate constant external disturbances. In a more recent work [18], a time-domain disturbance observer based control (DOBC) is implemented to improve the robustness of feedback linearization control with respect to external disturbances which is generated by Dryden wind turbulence model. The time domain disturbance observer presented can asymptotically estimate constant disturbances. However, a bounded estimation error is produced by the observer for time-

The project was supported under the Research University Grant No. Q.J130000.2608.14J62, Universiti Teknologi Malaysia.

Izzuddin M. Lazim, Abdul Rashid Husain, Mohd Ariffanan Mohd Basri and Nurul Adilla Mohd Subha are with the Department of Control and Mechatronics Engineering, School of Electrical Engineering, Faculty of Electrical Engineering, Universiti Teknologi Malaysia, 81310 Johor Bahru, Malaysia. (e-mail: nhizzuddin2@live.utm.my, abrashid@utm.my, ariffanan@fke.utm.my, nuruladilla@utm.my).

varying disturbances. Although higher observer bandwidth can reduce the estimation error, this can make the system susceptible to noise and poor transient performance [19].

In recent years, the application of artificial neural network (ANN) has become a promising research topic in control field due to the good approximation abilities, e.g. [20]–[22]. One of the popular ANN is the radial basis function neural network (RBFNN) that has a simple network and good generalization ability [23]. In [24], adaptive RBFNN is implemented to approximate mismatched uncertainties. In [25], an improved backstepping control using RBFNN is proposed to approximate unknown perturbations which shows promising results. In brief, these studies have proven the good approximation ability of RBFNN.

Motivated by the above studies, the main objective of our paper is to improve the disturbance observer-based feedback linearization control proposed in [18] by integrating DOBC with RBFNN, forming so-called intelligent DOBC (iDOBC). Using the good approximation ability of the RBFNN, bounded disturbance estimation error produced by the disturbance observer is approximated and compensated without using high observer bandwidth. We show that the proposed iDOBC, when integrated with state feedback (SF) control, forming SF-iDOBC can improve the trajectory tracking performance of quadrotor in the presence of time-varying wind disturbances. To the best of our knowledge, this study is the first to propose RBFNN for improving disturbance rejection capability of the DOBC.

The paper is organized as follows. Firstly, Section II presents the nonlinear quadrotor model. In Section III, control system designs are presented. Using the feedback linearization approach, linear decoupled equations with disturbance parts are obtained. For the quadrotor trajectory tracking, state-feedback control is presented in the outer-loop layer. To estimate the external disturbances affecting the quadrotor, time domain disturbance observer is described. Then, RBFNN is presented to improve the disturbance compensation by approximating the bounded estimation error produced by the disturbance observer. In Section IV, numerical simulation results and discussion are presented, followed by concluding remarks in Section V.

II. Nonlinear Quadrotor Model

Consider the configuration for a quadrotor as shown in Fig. 1 where (F_1, F_2, F_3, F_4) are the lift forces generated by the four rotors, while (x, y, z) and (ϕ, θ, ψ) denote the absolute position with respect to the earth frame F_e and orientation (roll, pitch, yaw) of the quadrotor, respectively. By considering the translational and rotational components, the 6-DOF nonlinear model of the quadrotor is given by [9]

$$\ddot{x} = \alpha\, u^{\{1\}}/m + T_x/m \tag{1}$$

$$\ddot{y} = \beta\, u^{\{1\}}/m + T_y/m \tag{2}$$

$$\ddot{z} = -a_g + \gamma\, u^{\{1\}}/m + T_z/m \tag{3}$$

$$\ddot{\phi} = \dot{\theta}\dot{\psi}\,(I_y - I_z)/I_x + u^{\{2\}}/I_x \tag{4}$$

$$\ddot{\theta} = \dot{\phi}\dot{\psi}\,(I_z - I_x)/I_y + u^{\{3\}}/I_y \tag{5}$$

$$\ddot{\psi} = \dot{\psi}\dot{\theta}\,(I_x - I_y)/I_z + u^{\{4\}}/I_z \tag{6}$$

where $\boldsymbol{u} = \left[u^{\{1\}}, u^{\{2\}}, u^{\{3\}}, u^{\{4\}}\right]^T$, m and a_g are the control inputs of the system, the mass of quadrotor, and the gravitational acceleration, respectively. Meanwhile, I_q and T_q $(q = x, y, z)$ denote, respectively the moment of inertia along each axis and the disturbing forces on the quadrotor due to the wind, and

$$\begin{aligned} \alpha &= c\phi s\theta cthe\ \psi + s\phi the\ the\ the\ s\psi \\ \beta &= c\phi s\theta s\psi - s\phi c\psi \\ \gamma &= c\phi c\theta \end{aligned} \tag{7}$$

with the terms $s(\cdot)$ and $c(\cdot)$ represent the sine and cosine functions, respectively.

The quadrotor is an underactuated and highly unstable nonlinear system which brings a challenge in the design of the control mechanism. One of the approaches used to simplify the dynamics of this system is by using feedback linearization technique.

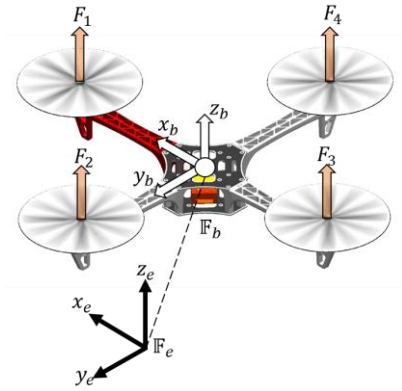

Fig. 1. The configuration of a quadrotor with the earth-fixed frame, $\mathbb{F}_e$ and body-fixed frame, $\mathbb{F}_b$.

III. Control System Design

This section presents the control system that makes the quadrotor track the desired reference trajectory despite the presence of external disturbances. The control system design, SF-iDOBC can be grouped into two loops; inner loop and outer loop. Firstly, the inner loop control that involves linearization of the quadrotor model using feedback linearization approach is described. In the outer loop control, linear state-feedback control is designed to stabilize the resulting linear model. Then, disturbance observer is derived to estimate the disturbance affecting the quadrotor flight based on the input-output signals of the linearized model. Finally, RBFNN is derived to estimate the bounded disturbance estimation error produced by the disturbance observer.

A. Feedback Linearization of Nonlinear Quadrotor Model

Nonlinear control using feedback linearization approach involves the transformation of nonlinear dynamics into the

equivalent linear system by coordinate transformation and nonlinear state feedback [8]. Fig. 2 illustrates the linearization of the quadrotor model using feedback linearization technique.

For linearizing the nonlinear quadrotor dynamics, the absolute position (x, y, z) and the yaw angle (ψ) are chosen as the outputs. To avoid singularity in Lie transformation matrices for feedback linearization, the real control signal $\boldsymbol{u}$ has been replaced by $\bar{\boldsymbol{u}} = \left[\bar{u}^{\{1\}}, \bar{u}^{\{2\}}, \bar{u}^{\{3\}}, \bar{u}^{\{4\}}\right]^T$. In this case, $u^{\{1\}}$ has been delayed by the double integrator, while other control signals remain unchanged [26].

$$\begin{aligned} \bar{u}^{\{1\}} &= \dot{\xi}, \;\; \dot{\zeta} = \xi, \;\; \zeta = u^{\{1\}} \\ \bar{u}^{\{2\}} &= u^{\{2\}} \\ \bar{u}^{\{3\}} &= u^{\{3\}} \\ \bar{u}^{\{4\}} &= u^{\{4\}} \end{aligned} \tag{8}$$

Then, the extended system of (1) - (6) is given as

$$\dot{\mathbf{x}} = \mathbf{f}(\mathbf{x}) + \sum_{j=1}^{4} \mathbf{g}_j(\mathbf{x}) \bar{u}^{\{j\}} \tag{9}$$

where $\mathbf{x} = \left[p_x, \dot{p}_x, p_y, \dot{p}_y, p_z, \dot{p}_z, \zeta, \xi, \phi, \dot{\phi}, \theta, \dot{\theta}, \psi, \dot{\psi}\right]^T \in \mathbb{R}^b$, $\mathbf{y} = [h_1, h_2, h_3, h_4]^T = [x, y, z, \psi]^T$, and

$$\begin{aligned} \mathbf{f}(\mathbf{x}) = \Bigg[& \dot{p}_x, \frac{(\alpha\zeta + T_x)}{m}, \dot{p}_y, \frac{(\beta\zeta + T_y)}{m}, \dot{p}_z, -a_g \\ & + \frac{(\gamma\zeta + T_z)}{m}, \xi, 0, \dot{\phi}, \frac{\dot{\theta}\dot{\psi}(I_y - I_z)}{I_x}, \dot{\theta}, \\ & \frac{\dot{\phi}\dot{\psi}(I_z - I_x)}{I_y}, \dot{\psi}, \frac{\dot{\psi}\dot{\theta}(I_x - I_y)}{I_z} \Bigg]^T, \end{aligned}$$

$$\mathbf{g}_1 = [0,0,0,0,0,0,0,1,0,0,0,0,0,0]^T,$$

$$\mathbf{g}_2 = \left[0,0,0,0,0,0,0,0,0,\frac{1}{I_x},0,0,0,0\right]^T,$$

$$\mathbf{g}_3 = \left[0,0,0,0,0,0,0,0,0,0,0,\frac{1}{I_y},0,0\right]^T,$$

$$\mathbf{g}_4 = \left[0,0,0,0,0,0,0,0,0,0,0,0,0,\frac{1}{I_z}\right]^T$$

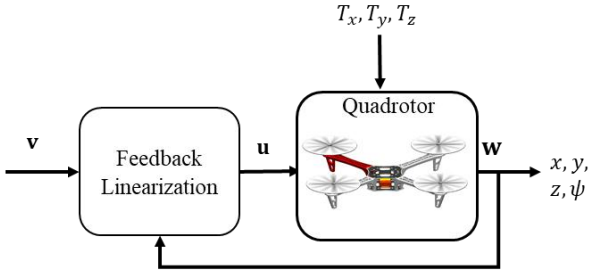

Fig. 2. Feedback linearization of the nonlinear quadrotor system.

For the nonlinear system (9), the relative degree $\{r_1, r_2, r_3, r_4\}$ is given by $r_1 = r_2 = r_3 = 4$ and $r_4 = 2$ and dimension $b = 14$. Therefore, the condition $\sum_{j=1}^{4} r_j = b$ is fulfilled, and the input-output decoupling problem is solvable for the system using the control input given as follows [10]:

$$\bar{\boldsymbol{u}} = \boldsymbol{\Delta}^{-1}(\mathbf{x})(-\mathbf{b}(\mathbf{x}) + \mathbf{v}) \tag{10}$$

with $\mathbf{v} = \left[v_x, v_y, v_z, v_\psi\right]^T$ is the vector of control inputs for the linearized model, and

$$\begin{aligned} \boldsymbol{\Delta}(\mathbf{x}) &= \begin{bmatrix} L_{g_1} L_f^{r_1 - 1} h_1(\bar{x}) & \cdots & L_{g_4} L_f^{r_1 - 1} h_1(\bar{x}) \\ \vdots & \ddots & \vdots \\ L_{g_1} L_f^{r_4 - 1} h_4(\bar{x}) & \cdots & L_{g_4} L_f^{r_4 - 1} \boldsymbol{h}_4(\bar{x}) \end{bmatrix} \\ &= \begin{bmatrix} \frac{\alpha}{m} & \frac{\zeta\Gamma}{mI_x} & \frac{\zeta\gamma c\psi}{mI_y} & -\frac{\zeta\beta}{mI_z} \\ \frac{\beta}{m} & -\frac{\zeta\Lambda}{mI_x} & \frac{\zeta\gamma s\psi}{mI_y} & \frac{\zeta\alpha}{mI_z} \\ \frac{\gamma}{m} & -\frac{\zeta s\phi c\theta}{mI_x} & -\frac{\zeta c\phi s\theta}{mI_y} & 0 \\ 0 & 0 & 0 & \frac{1}{I_z} \end{bmatrix} \end{aligned} \tag{11}$$

$$\mathbf{b}(\bar{x}) = \begin{bmatrix} L_f^{r_1} h_1(\mathbf{x}) \\ \vdots \\ L_f^{r_4} h_4(\mathbf{x}) \end{bmatrix} \tag{12}$$

with $\Gamma = c\phi s\psi - s\phi s\theta c\psi$ and $\Lambda = c\phi c\psi + s\phi s\theta s\psi$. $L_g^k h_j$ denotes the k-th Lie derivative of h_j along g.

For an exact feedback linearization without external disturbances (i.e. $T_q = 0$), equation (10) transforms (9) into four decoupled linear dynamics as follows:

$$\begin{aligned} \frac{d(\ddot{x})}{dt} &= v_x, \qquad \frac{d(\ddot{y})}{dt} = v_y \\ \frac{d(\ddot{z})}{dt} &= v_z, \qquad \frac{d(\dot{\psi})}{dt} = v_\psi \end{aligned} \tag{13}$$

However, equation (10) may not perfectly linearize the nonlinear quadrotor dynamics due to parametric uncertainties (e.g. mass and moments of inertia) and external disturbances (e.g. wind and load). Hence, the resultant feedback linearization using (10) consists of the nominal part and the unknown disturbance part, $\mathbf{d} = \left[d_x, d_y, d_z, d_\psi\right]^T$ given as follows:

$$\begin{aligned} \frac{d(\ddot{x})}{dt} &= v_x + d_x, \qquad \frac{d(\ddot{y})}{dt} = v_y + d_y \\ \frac{d(\ddot{z})}{dt} &= v_z + d_z, \qquad \frac{d(\dot{\psi})}{dt} = v_\psi + d_\psi \end{aligned} \tag{14}$$

Equation (14) can be re-written in state-space given as

$$\dot{\mathbf{w}}_j = \mathbf{A}_j \mathbf{w}_j + \mathbf{B}_j(v_j + d_j) \quad j \in \{x, y, z, \psi\} \tag{15}$$

where $\mathbf{w}_q = [q, \dot{q}, \ddot{q}, \dddot{q}]^T$ and $\mathbf{w}_\psi = \left[\psi, \dot{\psi}\right]^T$, while

$$\begin{aligned} \mathbf{A}_x = \mathbf{A}_y = \mathbf{A}_z &= \begin{bmatrix} 0 & 1 & 0 & 0 \\ 0 & 0 & 1 & 0 \\ 0 & 0 & 0 & 1 \\ 0 & 0 & 0 & 0 \end{bmatrix}, \\ \mathbf{A}_\psi &= \begin{bmatrix} 0 & 1 \\ 0 & 0 \end{bmatrix}, \\ \mathbf{B}_x = \mathbf{B}_y = \mathbf{B}_z &= [0\;0\;0\;1]^T, \\ \mathbf{B}_\psi &= [0\;1]^T \end{aligned}$$

B. State Feedback Control for Nominal Plant

To stabilize the feedback linearized model in (15) and track the desired trajectory, this paper adopted state-feedback control law given as

$$v_{o_j} = -\mathbf{K}_j \mathbf{w}_j + G_j R_j \tag{16}$$

where $\mathbf{K}_j$ is the feedback gain matrix, G_j is the feedforward gain, and R_j is the desired output trajectory. The nominal control law (16) is designed based on the ideal model without considering the influence of disturbances, i.e. $d_j = 0$.

By substituting (16) as the input of (15), the closed loop dynamics is given as

$$\begin{aligned} \dot{\mathbf{w}}_j &= \mathbf{A}_j \mathbf{w}_j + \mathbf{B}_j\left(-\mathbf{K}_j \mathbf{w}_j + G_j R_j + d_j\right) \\ &= \left(\mathbf{A}_j - \mathbf{B}_j \mathbf{K}_j\right)\mathbf{w}_j + G_j \mathbf{B}_j R_j + \mathbf{B}_j d_j \end{aligned} \tag{17}$$

Notice that the closed-loop dynamics using the nominal controller is influenced by the external disturbances d_j. In order to compensate for the disturbances, an improved compensation scheme using time-domain disturbance observer and RBFNN is presented in the next subsections.

C. Disturbance Observer

To estimate the disturbances, d_j in the system (15), the following time-domain disturbance observer is employed [18]:

$$\dot{Z}_j = -\mathbf{L}_j \mathbf{B}_j\left(Z_j + \mathbf{L}_j \mathbf{w}_j\right) - \mathbf{L}_j\left(\mathbf{A}_j \mathbf{w}_j + \mathbf{B}_j v_j\right), \tag{18}$$

$$\hat{d}_j = \mathbf{L}_j \mathbf{w}_j + Z_j \tag{19}$$

where Z_j is the internal variable of the observer, $\hat{d}_j$ is the estimated disturbance, and $\mathbf{L}_j$ is the observer gain matrix to be designed. Define the disturbance estimation error as the deviation between the actual and estimated disturbance, given as

$$e_{d_j} = d_j - \hat{d}_j \tag{20}$$

Differentiating e_{d_j} with respect to time and substituting with (15) and (18) - (20) yields

$$\begin{aligned} \dot{e}_{d_j} &= \dot{d}_j - \dot{\hat{d}}_j \\ &= -\mathbf{L}_j \mathbf{B}_j e_{d_j} + \dot{d}_j \end{aligned} \tag{21}$$

The observer gain matrix, $\mathbf{L}_j$ is designed as

$$\mathbf{L}_j = L_{d_j} \mathbf{B}_j^{+} \tag{22}$$

where $\mathbf{B}_j^{+}$ denotes the pseudo-inverse of the matrix $\mathbf{B}_j$, and $L_{d_j} > 0$. Thus, the error dynamics of disturbance estimation in (21) becomes

$$\dot{e}_{d_j} = -L_{d_j} e_{d_j} + \dot{d}_j \tag{23}$$

Therefore, the disturbance estimation error in (23) is BIBO stable if the observer gain $L_{d_j} > 0$. The solution of the error dynamics in (23) is given as follows:

$$e_{d_j} = \mathrm{e}^{-L_{d_j} t}\, e_{d_j}(0) + \int_0^t \mathrm{e}^{-L_{d_j}(t-\tau)} \dot{d}_j(\tau) d\tau \tag{24}$$

with e is the exponential function and t is the time variable. For constant disturbances (i.e. $\dot{d}_j = 0$), the estimation error e_{d_j} converges to zero asymptotically. Meanwhile for bounded disturbance derivative $\left(\dot{d}_j(t) < \rho_j\right)$ and bounded initial estimation error $\left(e_{d_j}(0) < \lambda_j\right)$, the disturbance estimation error is also bounded $\left(e_{d_j} < \varpi_j\right)$ for $t \geq 0$.

In this paper, we proposed a method to attenuate the bounded disturbance estimation error using RBFNN as presented in the next subsection.

D. Compensation of Disturbance Estimation Error using RBFNN

Since the nominal controller in (16) cannot reject the external disturbances, a new control algorithm to attenuate the disturbances which composed of disturbance observer and RBFNN is proposed in this paper given as follows:

$$v_j = v_{o_j} - \hat{d}_j - v_{nn_j} \tag{25}$$

where v_{o_j} is the nominal controller in eq. (16), $\hat{d}_j$ is the estimated disturbance in (19), and v_{nn_j} is the compensation of the bounded disturbance estimation error using RBFNN, which is derived in this section.

By substituting the proposed controller (25) into the plant in (15), the closed-loop dynamics is given as

$$\begin{aligned} \dot{\mathbf{w}}_j &= \mathbf{A}_j \mathbf{w}_j + \mathbf{B}_j\left(v_j + d_j\right) \\ &= \left(\mathbf{A}_j - \mathbf{B}_j \mathbf{K}_j\right)\mathbf{w}_j + G_j \mathbf{B}_j R_j + \mathbf{B}_j\left(d_j - \hat{d}_j\right) \\ &\qquad - \mathbf{B}_j v_{nn_j} \\ &= \left(\mathbf{A}_j - \mathbf{B}_j \mathbf{K}_j\right)\mathbf{w}_j + G_j \mathbf{B}_j R_j + \mathbf{B}_j\left(e_{d_j} - v_{nn_j}\right) \end{aligned} \tag{26}$$

To form an error signal representing the deviation of the true plant response caused by the disturbance estimation error, a reference model representing the ideal closed-loop dynamics is introduced as follows:

$$\begin{aligned} \dot{\mathbf{w}}_{m_j} &= \mathbf{A}_j \mathbf{w}_{m_j} + \mathbf{B}_j v_{o_j} \\ &= \left(\mathbf{A}_j - \mathbf{B}_j \mathbf{K}_j\right)\mathbf{w}_{m_j} + G_j \mathbf{B}_j R_j \end{aligned} \tag{27}$$

where $\mathbf{w}_{m_j}$ is the state of the reference model. An error between the closed-loop plant and the reference model is formed when both dynamics are fed with the same reference signal, R_j. This error is defined as

$$\boldsymbol{e}_j = \mathbf{w}_j - \mathbf{w}_{m_j} \tag{28}$$

Therefore, the error dynamics between the closed-loop plant and reference model is obtained by differentiating (28) and substituting with (26) and (27) as follows:

$$\dot{\boldsymbol{e}}_j = \left(\mathbf{A}_j - \mathbf{B}_j \mathbf{K}_j\right)\boldsymbol{e}_j + \mathbf{B}_j\left(e_{d_j} - v_{nn_j}\right) \tag{29}$$

Since $\mathbf{K}_j$ is chosen such that matrix $\mathbf{A}_j - \mathbf{B}_j \mathbf{K}_j$ is Hurwitz, there exists a real symmetric positive definite matrix $\mathbf{P}_j$

satisfying

$$(\mathbf{A}_j - \mathbf{B}_j\mathbf{K}_j)^T\mathbf{P}_j + \mathbf{P}_j(\mathbf{A}_j - \mathbf{B}_j\mathbf{K}_j) = -\mathbf{Q}_j \quad (30)$$

where $\mathbf{Q}_j$ is a positive definite matrix which is chosen by the designer.

In this paper, RBFNN is employed to approximate and attenuate the unknown bounded disturbance estimation error, $e_{d_j} < \varpi_j$. Structure of a typical RBFNN is shown in Fig. 3 which consists of three layers: an input layer, a hidden layer, and an output layer.

In the input layer, $\boldsymbol{e}_j$ which is the error between the states of the closed-loop plant and the reference model is selected as the RBFNN input.

The hidden layer comprises of l number of neurons with a nonlinear Gaussian activation function given as

$$S_{j_i}(\boldsymbol{e}_j) = \exp\left(-\frac{\|\boldsymbol{e}_j - \boldsymbol{\mu}_{j_i}\|}{\eta_j^2}\right), \qquad i = 1,2,\cdots,l \quad (31)$$

where $\boldsymbol{\mu}_{j_i} = [\mu_{j_1},\cdots,\mu_{j_l}]^T$ and η_j are the centers and width of the Gaussian function, respectively.

The RBFNN approximation of e_{d_j} is calculated in the output layer using the weighted sum function given as

$$v_{nn_j} = \boldsymbol{\Theta}_j^T\mathbf{S}_j \quad (32)$$

with $\boldsymbol{\Theta}_j = [\Theta_{j_1},\cdots\Theta_{j_l}]^T \in \mathbb{R}^l$ is the weight vector, and $\mathbf{S}_j = [S_{j_1}\cdots S_{j_l}]^T \in \mathbb{R}^l$.

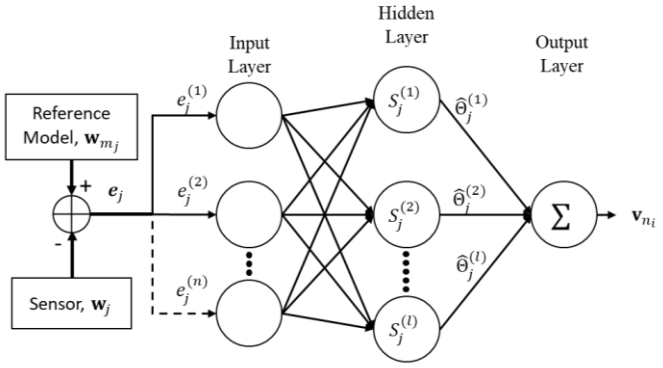

Fig. 3. Structure of the proposed radial basis function neural network (RBFNN)

Based on the universal approximation ability of RBFNN [27], there exists an optimal RBFNN to learn the unknown disturbance estimation error, e_{d_j} over a compact region $\varpi_j \in \mathbb{R}^n$ such that

$$e_{d_j} = \boldsymbol{\Theta}^{*T}_j\mathbf{S}_j + \epsilon_j \quad (33)$$

with ϵ_j is the approximation error of RBFNN. The optimal weight vector $\boldsymbol{\Theta}_j^*$ is defined as

$$\boldsymbol{\Theta}_j^* = \arg\min_{\boldsymbol{\Theta}\in\mathbb{R}^l}\left\{\sup_{\boldsymbol{e}_j\in\varpi_j}\left|e_{d_j}(\boldsymbol{e}_j) - v_{nn_j}(\boldsymbol{e}_j)\right|\right\} \quad (34)$$

By substituting (32) and (33) into (29) yields

$$\dot{\boldsymbol{e}}_j = (\mathbf{A}_j - \mathbf{B}_j\mathbf{K}_j)\boldsymbol{e}_j + \mathbf{B}_j(\tilde{\boldsymbol{\Theta}}_j^T\mathbf{S}_j + \epsilon_j) \quad (35)$$

where $\tilde{\boldsymbol{\Theta}}_j = \boldsymbol{\Theta}_j^* - \boldsymbol{\Theta}_j$. Lyapunov based approach was implemented to find the weight adaptation law given as

$$\dot{\boldsymbol{\Theta}}_j = \lambda_j\mathbf{S}_j\boldsymbol{e}_j^T\mathbf{P}_j\mathbf{B}_j \quad (36)$$

with $\lambda_j > 0$ is an adaptation gain to be designed. Block diagram of the proposed control approach is illustrated in Fig. 4

Assumption 1: Approximation error of RBFNN, ϵ_j is zero. This assumption will hold for comparatively less complex functions with a sufficiently large number of adjustable weight [28].

Theorem 1: For the nonlinear quadrotor system (1) - (6) which is linearized using (10) and yields (15), consider control law (25) with (19) and (32), and adaptation law (36). If Assumption 1 is satisfied, then, the proposed controller SF-iDOBC guarantees

$$\lim_{t\to\infty}\boldsymbol{e}_j(t) = 0 \quad (37)$$

Proof:
Consider the following Lyapunov candidate:

$$V_j = \frac{1}{2}\boldsymbol{e}_j^T\mathbf{P}_j\boldsymbol{e}_j + \frac{1}{2\lambda_j}\mathrm{tr}\{\tilde{\boldsymbol{\Theta}}_j^T\tilde{\boldsymbol{\Theta}}_j\} \quad (38)$$

where $\mathrm{tr}\{\cdot\}$ is the trace operator of matrix algebra. Differentiating (38) with respect to time and substituting with (30) and (35) yields:

$$\begin{aligned}\dot{V}_j &= \frac{1}{2}(\dot{\boldsymbol{e}}_j^T\mathbf{P}_j\boldsymbol{e}_j + \boldsymbol{e}_j^T\mathbf{P}_j\dot{\boldsymbol{e}}_j) + \frac{1}{\lambda_j}\mathrm{tr}\left\{\dot{\tilde{\boldsymbol{\Theta}}}_j^T\tilde{\boldsymbol{\Theta}}_j\right\}\\ &= -\frac{1}{2}\boldsymbol{e}_j^T\mathbf{Q}_j\boldsymbol{e}_j + \mathbf{S}_j^T\tilde{\boldsymbol{\Theta}}_j\mathbf{B}_j^T\mathbf{P}_j\boldsymbol{e}_j + \epsilon_j\mathbf{B}_j^T\mathbf{P}_j\boldsymbol{e}_j\\ &\quad + \frac{1}{\lambda_j}\mathrm{tr}\left\{\dot{\tilde{\boldsymbol{\Theta}}}_j^T\tilde{\boldsymbol{\Theta}}_j\right\}\end{aligned} \quad (39)$$

By noting that $\mathbf{S}_j^T\tilde{\boldsymbol{\Theta}}_j\mathbf{B}_j^T\mathbf{P}_j\boldsymbol{e}_j = \mathrm{tr}\{\mathbf{B}_j^T\mathbf{P}_j\boldsymbol{e}_j\mathbf{S}_j^T\tilde{\boldsymbol{\Theta}}_j\}$, and $\dot{\tilde{\boldsymbol{\Theta}}}_j = -\dot{\boldsymbol{\Theta}}_j$, (39) becomes

$$\begin{aligned}\dot{V}_j &= -\frac{1}{2}\boldsymbol{e}_j^T\mathbf{Q}_j\boldsymbol{e}_j + \frac{1}{\lambda_j}(\lambda_j\mathbf{B}_j^T\mathbf{P}_j\boldsymbol{e}_j\mathbf{S}_j^T - \dot{\boldsymbol{\Theta}}_j^T)\tilde{\boldsymbol{\Theta}}_j\\ &\quad + \epsilon_j^T\mathbf{B}_j^T\mathbf{P}_j\boldsymbol{e}_j\end{aligned} \quad (40)$$

By substituting adaptation law (36) in (40) yields:

$$\dot{V}_j = -\frac{1}{2}\boldsymbol{e}_j^T\mathbf{Q}_j\boldsymbol{e}_j + \boldsymbol{e}_j^T\mathbf{P}_j\mathbf{B}_j\epsilon_j \quad (41)$$

Therefore, based on Assumption 1, $\dot{V}_j < 0$. This completes the proof.

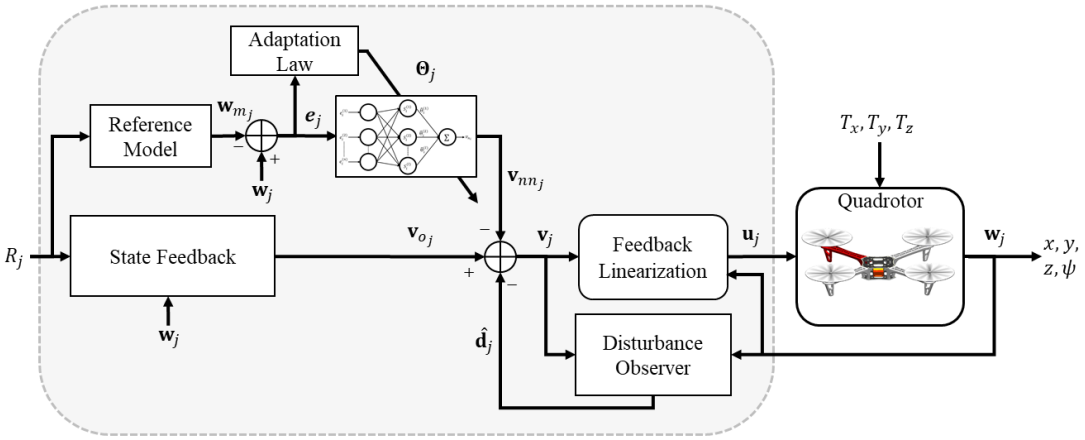

Fig. 4. Block diagram of the proposed control method.

IV. Simulation Results and Discussion

In this section, the performance of the proposed control method is evaluated. The corresponding control algorithm and quadrotor model are implemented in Matlab/Simulink simulation environment.

The parameters in [9] are adopted for the quadrotor model with $m = 0.6$ kg, $I_x = I_y = 0.005796\ \text{kg}\cdot\text{m}^2, I_z = 0.010296\text{kg}\cdot\text{m}^2$ and $a_g = 9.81\text{ms}^{-2}$. The gains for the state feedback control law and disturbance observer are $\mathbf{K}_x = \mathbf{K}_y = \mathbf{K}_z = [16\ 32\ 24\ 8]$, $\mathbf{K}_\psi = [1\ 2]$, $G_x = G_y = G_z = 16$, $G_\psi = 1$, and $L_{d_j} = 10$. For compensating the error in the disturbance estimation of d_q, the RBFNN uses four, five and one (4-5-1) neurons at the input, hidden and output layers, respectively. Meanwhile, RBFNN with two input neurons, five hidden neurons, and one output neurons (2-5-1) are used to compensate the disturbance estimation error of d_ψ. The centers of the neurons are spaced evenly in the interval $[-2, 2]$. The widths of Gaussian functions are $\eta_j = 5$ with adaptation gain $\lambda_j = 1000$. Matrix $\mathbf{P}_j$ is obtained using (30) by setting $\mathbf{Q}_x = \mathbf{Q}_y = \mathbf{Q}_z = [1,1,1,1]$ and $\mathbf{Q}_\psi = [1,1]$.

To test the effectiveness of the proposed control algorithm, two simulation experiments have been carried out on the quadrotor in the influence of external disturbances. Dryden wind gust model [29] is used to simulate the effect of aerodynamic forces on the quadrotor. Fig. 5 shows the generated forces in longitudinal and lateral directions.

The simulation results are presented in the following subsections. As a benchmark, the performance of the proposed controller is compared with the results obtained by using the linear state feedback control law with disturbance observer (SF-DOBC), proposed in [18]. The quantitative performances are measured using integral absolute error (*IAE*) given as follows:

$$IAE = \int_0^{T_s} |E(t)|\, dt \tag{42}$$

with T_s is the period of the simulation, and E is the error between the desired and actual value.

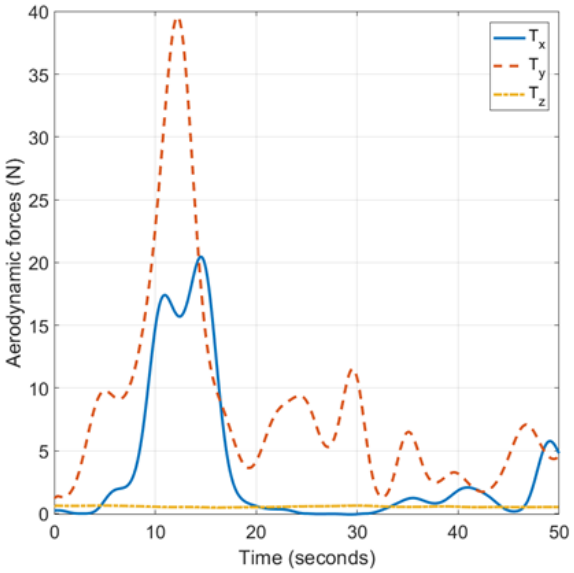

Fig. 5. Disturbances in longitudinal and lateral directions.

A. Simulation Experiment 1: Quadrotor Hovering Subject to Wind Disturbances

Hover is one of the basic maneuvers for a quadrotor. In this simulation experiment, the quadrotor was required to hover at a constant desired position in the presence of time-varying aerodynamic forces produced by the wind disturbances.

The desired hovering position was set at $[R_x, R_y, R_z] = [1, -1, 2]m$ and $R_\psi = 0rad$. The initial position of the quadrotor was $[x(0), y(0), z(0)] = [0,0,0]m$ and $\psi(0) = \pi/4rad$. Other states were set to zero. From the initial position, the quadrotor then flew to the desired fixed position and hover at the point. The ability to hover at this position in the presence of wind disturbance was studied in this simulation experiment.

The proposed controller in (25) was implemented to ensure the quadrotor able to hover at the desired position in the presence of the external disturbances. As a benchmark, the performance of the quadrotor hovering using the proposed controller was compared with the results obtained by using SF-DOBC, proposed in [18]. The results of the simulation

experiment are shown in Fig. 6 - Fig. 7.

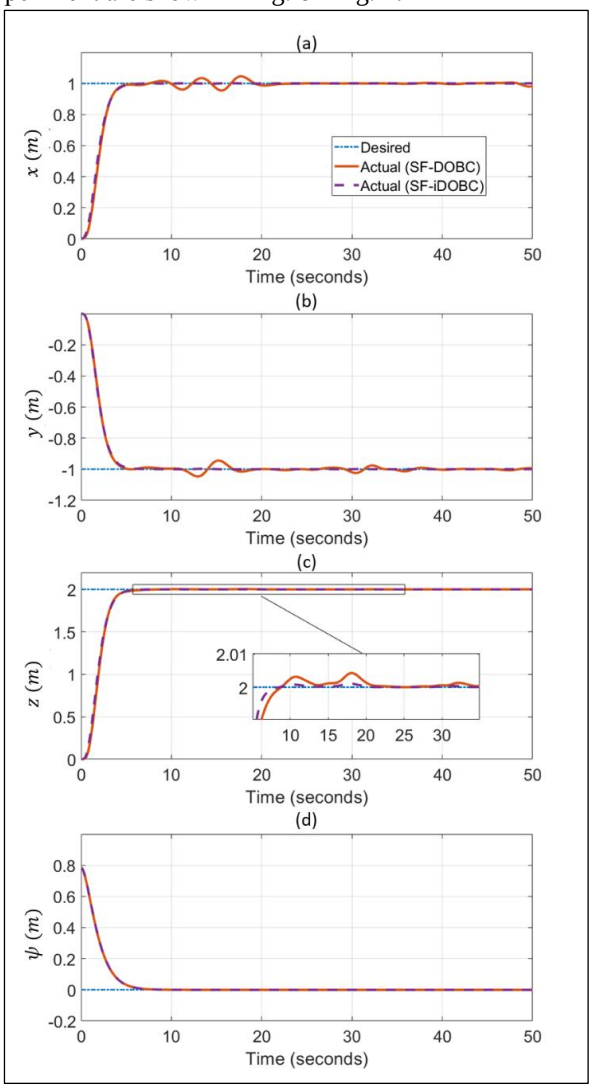

Fig. 6. Time response of the hovering quadrotor.

In Fig. 6, the time response of the hovering quadrotor is shown. It can be seen from the figure that the quadrotor can track the desired signals from the initial position to the desired hovering point using SF-DOBC and SF-iDOBC. However, there were some deviations in the quadrotor's translational (x, y, z) motion using SF-DOBC during hovering due to the wind disturbances.

On the other hand, the quadrotor with SF-iDOBC shows good hovering control despite the presence of wind disturbances. This is verified through quantitative analysis using *IAE* tabulated in Table I. Notice that the performance of both controllers for heading (ψ) were identical as no aerodynamic moments disturbance is considered. The corresponding control inputs are shown in Fig. 7.

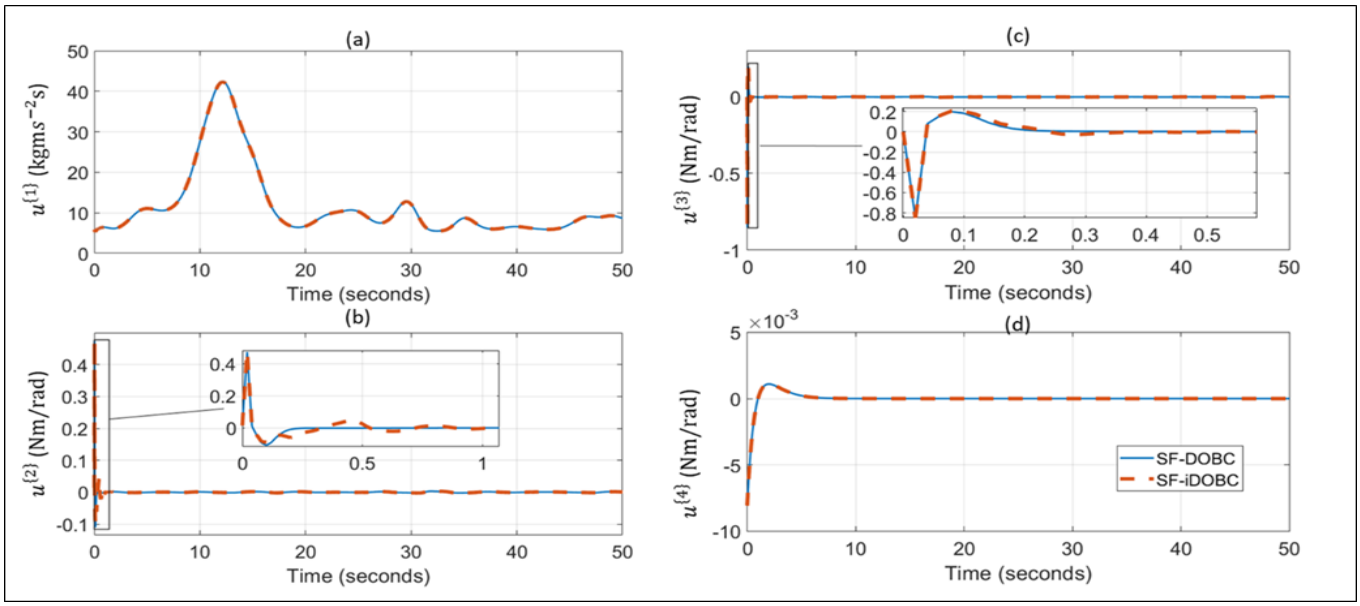

Fig. 7. Control signal of the hovering quadrotor.

TABLE I
Quantitative comparison between SF-DOBC and SF-iDOBC for quadrotor hovering problem.

Controller	*IAE*			
	x	y	z	ψ
SF-DOBC	2.419	2.370	4.186	1.571
SF-iDOBC	1.984	2.016	4.023	1.571
Reduction (%)	17.982	14.937	3.894	0.000

B. Simulation experiment 2: Quadrotor Trajectory Tracking Subject to Wind Disturbances

To further demonstrate the capability of the proposed control scheme, a time-varying trajectory tracking of the quadrotor was simulated. This simulation study emphasizes the practical ability of the quadrotor to track a given time-varying desired trajectory while rejecting wind disturbances. The wind disturbances in Fig. 5 was implemented for the simulation study, while the following command was used to generate the desired circle trajectory:

$$\begin{aligned} R_x(t) &= 2\sin(0.1257t) \\ R_y(t) &= 2\sin\left(0.1257t + \frac{\pi}{2}\right) \\ R_z(t) &= 2 \\ R_\psi(t) &= 0 \end{aligned} \tag{43}$$

Initially, the quadrotor was positioned at $[x(0), y(0), z(0)] = [0, 0, 2]m$, with heading $\psi(0) = \pi/4rad$. Fig. 8 - Fig. 9 show the simulation results for circular time-varying trajectory tracking in the presence of wind disturbances using SF-DOBC and SF-iDOBC, respectively.

As can be seen in Fig. 8, the quadrotor trajectory using SF-DOBC is not smooth due to the wind disturbances. In contrast, quadrotor trajectory using SF-iDOBC is smooth despite the presence of wind disturbances as shown in Fig. 9. This is supported by the quantitative analysis using *IAE* performance index tabulated in Table II.

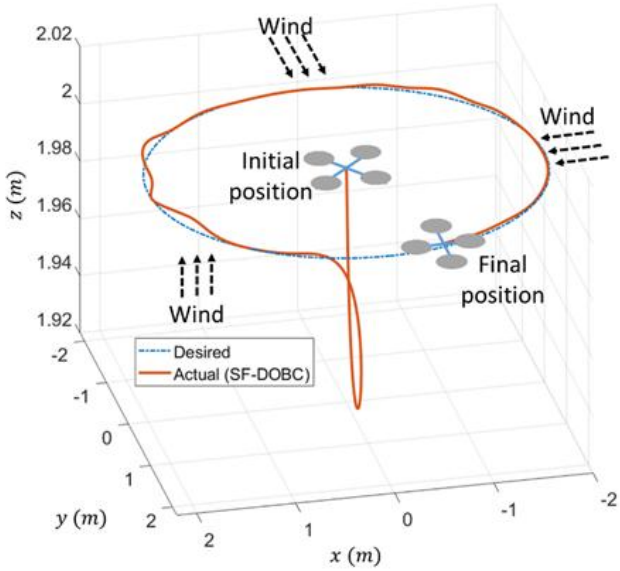

Fig. 8. 3D position circle trajectory tracking response using SF-DOBC.

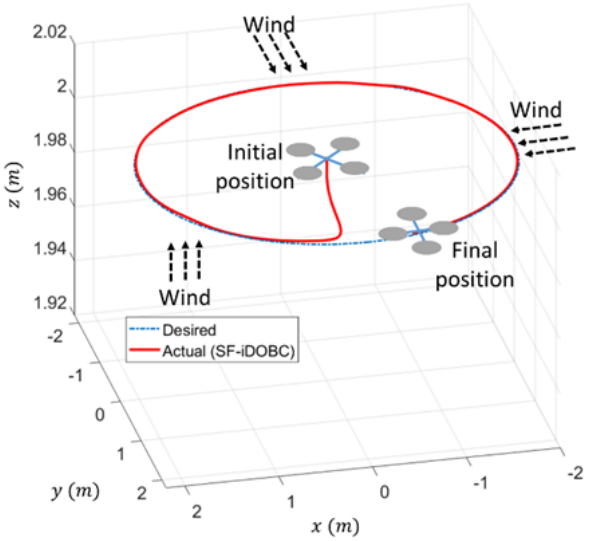

Fig. 9. 3D position circle trajectory tracking response using SF-iDOBC.

TABLE II
Quantitative comparison between SF-DOBC and SF-iDOBC for quadrotor hovering problem.

Controller	*IAE*			
	x	y	z	ψ
SF-DOBC	15.350	19.500	0.188	1.571
SF-iDOBC	15.240	19.200	0.031	1.571
Reduction (%)	0.717	1.538	83.511	0.000

V. Conclusion

In this paper, an enhanced disturbance observer is proposed to improve the robustness of autonomous quadrotor flight despite the presence of wind disturbances. This is achieved by using RBFNN to estimate the bounded disturbance estimation error produced by the standard disturbance observer. Using Dryden wind gust model to simulate the wind disturbance effect on a quadrotor, two simulation studies are carried out; quadrotor hovering and trajectory tracking. Simulation results show improvements in the autonomous quadrotor flight using the proposed control. Future research directions may include the deployment of the proposed control approach on experimental hardware and optimal selection of RBFNN centers using clustering algorithms.

Acknowledgment

The first author would like to thank the Ministry of Higher Education (MOHE) and Universiti Sains Islam Malaysia (USIM) for their financial support under SLAB scheme, and all the authors acknowledge the support by Universiti Teknologi Malaysia in term of lab facilities. The project is supported under the Research University Grant No. Q.J130000.2608.14J62, Universiti Teknologi Malaysia.

References

[1] I. M. Lazim, A. R. Husain, N. A. M. Subha, Z. Mohamed, and M. A. Mohd Basri, "Optimal Formation Control of Multiple Quadrotors

Based on Particle Swarm Optimization," in *Asian Simulation Conference*, 2017, pp. 121–135.

[2] M. A. M. Basri, A. R. Husain, and K. A. Danapalasingam, "A hybrid optimal backstepping and adaptive fuzzy control for autonomous quadrotor helicopter with time-varying disturbance," *Proc. Inst. Mech. Eng. Part G J. Aerosp. Eng.*, vol. 229, no. 12, pp. 2178–2195, 2015.

[3] A. L. Salih, M. Moghavvemi, H. A. F. Mohamed, and K. S. Gaeid, "Modelling and PID controller design for a quadrotor unmanned air vehicle," in *2010 IEEE International Conference on Automation Quality and Testing Robotics (AQTR)*, 2010, vol. 1, pp. 1–5.

[4] T. Sangyam, P. Laohapiengsak, W. Chongcharoen, and I. Nilkhamhang, "Path tracking of UAV using self-tuning PID controller based on fuzzy logic," in *Proceedings of SICE Annual Conference 2010*, 2010, pp. 1265–1269.

[5] A. Dharmawan, T. K. Priyambodo, and others, "Model of Linear Quadratic Regulator (LQR) Control Method in Hovering State of Quadrotor," *J. Telecommun. Electron. Comput. Eng.*, vol. 9, no. 3, pp. 135–143, 2017.

[6] K. T. Oner, E. Cetinsoy, M. Unel, M. F. Aksit, I. Kandemir, and K. Gulez, "Dynamic Model and Control of a New Quadrotor Unmanned Aerial Vehicle with Tilt-Wing Mechanism," 2008.

[7] M. A. B. M. Basri, "Intelligent Backstepping Control of Quadrotor Unmanned Aerial Vehicle," Universiti Teknologi Malaysia, 2015.

[8] M. A. Henson and D. E. Seborg, "Feedback Linearizing Control," in *Nonlinear Process Control*, no. 1, Upper Saddle River, NJ, USA: Prentice-Hall, Inc., 1997, pp. 149–232.

[9] A. Mahmood and Y. Kim, "Leader-following formation control of quadcopters with heading synchronization," *Aerosp. Sci. Technol.*, vol. 47, pp. 68–74, 2015.

[10] V. Mistler, A. Benallegue, and N. K. M'Sirdi, "Exact linearization and noninteracting control of a 4 rotors helicopter via dynamic feedback," in *Proceedings 10th IEEE International Workshop on Robot and Human Interactive Communication*, 2001, pp. 586–593.

[11] F. Sabatino, "Quadrotor control : modeling, nonlinear control design, and simulation," KTH Royal Institute of Technology, 2015.

[12] A. Mahmood and Y. Kim, "Decentralized formation control of quadcopters using feedback linearization," in *2015 6th International Conference on Automation, Robotics and Applications (ICARA)*, 2015, pp. 537–541.

[13] I. H. Choi and H. C. Bang, "Quadrotor-tracking controller design using adaptive dynamic feedback-linearization method," *Proc. Inst. Mech. Eng. Part G J. Aerosp. Eng.*, vol. 228, no. 12, pp. 2329–2342, 2014.

[14] W. Zhao and T. H. Go, "Quadcopter formation flight control combining MPC and robust feedback linearization," *J. Franklin Inst.*, vol. 351, no. 3, pp. 1335–1355, 2014.

[15] S. Li, J. Yang, W. H. Chen, and X. Chen, *Disturbance Observer-Based Control: Methods and Applications*. Boca Raton, Florida: CRC Press, 2014.

[16] A. Benallegue, A. Mokhtari, and L. Fridman, "Feedback linearization and high order sliding mode observer for a quadrotor UAV," in *International Workshop on Variable Structure Systems, 2006. VSS'06.*, 2006, pp. 365–372.

[17] A. Mokhtari, N. K. M'Sirdi, K. Meghriche, and A. Belaidi, "Feedback linearization and linear observer for a quadrotor unmanned aerial vehicle," *Adv. Robot.*, vol. 20, no. 1, pp. 71–91, 2006.

[18] A. Aboudonia, A. El-Badawy, and R. Rashad, "Disturbance observer-based feedback linearization control of an unmanned quadrotor helicopter," *Proc. Inst. Mech. Eng. Part I J. Syst. Control Eng.*, vol. 230, no. 9, pp. 877–891, 2016.

[19] J. S. Bay, *Fundamentals of Linear State Space Systems*. WCB/McGraw-Hill, 1999.

[20] M. Sharma and A. J. Calise, "Neural-Network Augmentation of Existing Linear Controllers," *J. Guid. Control. Dyn.*, vol. 28, no. 1, pp. 12–19, Jan. 2005.

[21] S. S. A. Ali, M. Moinuddin, K. Raza, and S. H. Adil, "An Adaptive Learning Rate for RBFNN Using Time-Domain Feedback Analysis," *The Scientific World Journal*, vol. 2014. 2014.

[22] H. Sun, L. Hou, and Y. Li, "Disturbance observer based dynamic surface tracking control for a class of uncertain nonlinear systems with mismatched disturbances," in *2016 12th World Congress on Intelligent Control and Automation (WCICA)*, 2016, pp. 605–610.

[23] J. Liu, *Radial Basis Function (RBF) Neural Network Control for Mechanical Systems*, vol. 53, no. 9. 2013.

[24] M. M. Arefi, M. R. Jahed-Motlagh, and H. R. Karimi, "Adaptive Neural Stabilizing Controller for a Class of Mismatched Uncertain Nonlinear Systems by State and Output Feedback," *IEEE Trans. Cybern.*, vol. 45, no. 8, pp. 1587–1596, Aug. 2015.

[25] M. A. M. Basri, K. A. Danapalasingam, and A. R. Husain, "Intelligent adaptive backstepping control for MIMO uncertain non-linear quadrotor helicopter systems," *Trans. Inst. Meas. Control*, vol. 37, no. 3, pp. 345–361, 2015.

[26] H. Wang and M. Chen, "Sliding mode attitude control for a quadrotor micro unmanned aircraft vehicle using disturbance observer," in *Proceedings of 2014 IEEE Chinese Guidance, Navigation and Control Conference*, 2014, pp. 568–573.

[27] T. Chen and H. Chen, "Approximation capability to functions of several variables, nonlinear functionals, and operators by radial basis function neural networks," *IEEE Trans. Neural Networks*, vol. 6, no. 4, pp. 904–910, Jul. 1995.

[28] L. Behera and I. Kar, *Intelligent Systems and Control: Principles and Applications*. New Delhi, India: Oxford University Press, 2010.

[29] S. Waslander and C. Wang, "Wind Disturbance Estimation and Rejection for Quadrotor Position Control," in *AIAA Infotech@Aerospace Conference*, 2009.